Journal Name

Chemical Science

Dynamic Article Links ▶

ARTICLE TYPE

Controlling the Self-Assembly of Cationic Bolaamphiphiles: Hydrotropic Counteranions Determine Aggregated Structures

Guanglu Wu,[a] Joice Thomas,[b] Mario Smet,[b] Zhiqiang Wang[a] and Xi Zhang*[a]

The role of hydrotropic counteranions in governing the self-assembled structures of cationic bolaamphiphiles is studied in this work. We reveal that the ability of a hydrotropic counteranion to induce the formation of two-dimensional (2D) planar aggregates depends weakly on its polar head, but is strongly correlated to the size and the substituted pattern of its organic portion. Additionally, the shape of 10 the obtained 2D planar aggregates can be modulated, interestingly, both by hydrotropic counteranions and the embedded conjugated moieties. 2D planar aggregates with a shape of triangle, quadrangle, and hexagon are obtained, which may provide a simple and feasible methodology for fabricating organic self-assembled structures with controlled features.

Introduction

15 Bolaamphiphiles, two hydrophilic heads connected by one hydrophobic skeleton, are kind of useful building blocks for self-assembly.[1–4] Due to its specific bipolar structure, the temperature to induce phase transition in the assemblies formed by bolaamphiphiles is higher than that of the conventional 20 amphiphiles.[5] Therefore, many archaebacteria containing high percentage of bolaamphiphiles are able to survive in a harsh environment.[6,7] Inspired by natural bolaamphiphiles, diversified artificial bolaamphiphiles with tailor-made architectures[8–15] and features[16–22] have been documented, which have enriched the 25 realm of molecular engineering of functional supramolecular systems. However, controlling the self-assembly of bolaamphiphiles in a facile manner remains a big challenge.

Our recent work demonstrated that the tosylate ion as counteranion for cationic bolaamphiphiles could lead to the 30 formation of two-dimensional (2D) planar aggregates,[23–25] while common counteranions like halide ions could only lead to one-dimensional (1D) or zero-dimensional (0D) aggregates.[26,27] The tosylate ion belongs to a class of ions denoted as hydrotropic anions, possessing both a hydrophobic part and a hydrophilic-35 polar-head, which are used to solubilize hydrophobic compounds into aqueous solution.[28,29] Utilized as counteranions in conventional cationic amphiphiles such as cetyltrimethylammonium, hydrotropic anions were able to modulate the properties of amphiphilic solutions including 40 critical micelle concentration, viscosity, ionization degree, and morphology.[30–34] In the self-assembly of cationic bolaamphiphiles, we wonder whether the formation of 2D planar aggregates would be specific for tosylate or general for hydrotropic anions, and whether there is rule behind the effect of 45 hydrotropic anions.

Herein, this paper is aimed to reveal the role of hydrotropic anions over the self-assembled structures of cationic bolaamphiphiles. By incorporating a diaryldiketopyrrolopyrrole (DPP) as the chromophore into the cationic bolaamphiphiles and 50 employing various hydrotropic anions as counteranions, we have attempted to establish the relationship between the molecular structures of hydrotropic anions and their ability to induce the formation of 2D planar aggregates. We have demonstrated clearly that the hydrophobicity of hydrotropic counteranions, including 55 the size of organic segments and the substituted pattern, determines the aggregated structure. Moreover, the shape of the obtained 2D planar aggregates can be modulated, interestingly, both by hydrotropic counteranions and the embedded conjugated moieties. 2D planar aggregates with a shape of triangle, 60 quadrangle, and hexagon are obtained, which may provide a simple and feasible methodology for fabricating organic self-assembled structures with controlled features.

Result and Discussion
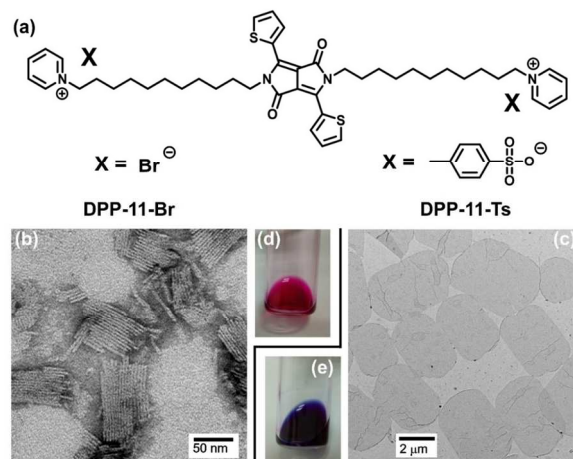
Fig. 1 Cationic bolaamphiphiles bearing different counterions, DPP-11-X (X = Br, Ts), lead to different self-assembled morphology as well as distinctive color of solution. (a) Molecular structures of DPP-11-X. (b) 1D rod-like structure of DPP-11-Br, and (c) 2D planar structure of DPP-
5 11-Ts observed by TEM. The colors of DPP-11-Br and DPP-11-Ts aqueous solutions are (d) light pink, and (e) dark blue, respectively. The concentrations of testing samples are both 2 mM. Testing temperature is 25 °C.

DPP-11-Br and DPP-11-Ts are two cationic bolaamphiphiles, as
10 shown in Fig 1a, which contain the same skeleton structure but employ bromide and tosylate as counteranions, respectively. Only a difference on counteranions is found to induce amazing differences on the properties of these two cationic bolaamphiphiles. Observed from transmission electron
15 microscopy (TEM), as shown in Fig. 1b-c, DPP-11-Br is found to form 1D rod-like aggregates with a width of 3.2 ± 0.1 nm and a length of ca. 70 nm; while DPP-11-Ts is found to form 2D planar aggregates with a width and a length on microscale. Additionally, DPP-11-Br and DPP-11-Ts show notable difference not only on
20 their self-assembled morphologies, but, more interestingly, on their color of solutions, as shown in Figure 1d-e. Under the same concentration, DPP-11-Br solution displays light pink; while DPP-11-Ts solution exhibits dark blue.
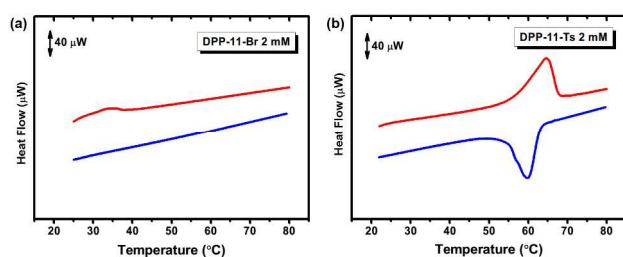
25 **Fig. 2** The DSC of DPP-11-Br solution (a) and DPP-11-Ts solution (b). The second heating and the first cooling curves are shown here. The concentrations of testing aqueous solutions are both 2 mM.

The aggregates of DPP-11-Br and DPP-11-Ts can both be dissociated at certain higher temperature. However, the
30 dissociation temperature and heat of the solutions of these two compounds are extremely different. As shown from differential scanning calorimeter (DSC) in Fig. 2, the aggregates of DPP-11-Br are dissociated at around 30 °C exhibiting a small and broad endothermic signal; while the dissociation point of DPP-11-Ts is
35 at 63 °C exhibiting a sharp endothermic peak. This high dissociation temperature suggests the existence of highly ordered molecular arrangement in the 2D planar structure of DPP-11-Ts; and moreover, the sharp endothermic peaks suggest the existence of strong association interactions between these highly-ordered
40 arranged building blocks.
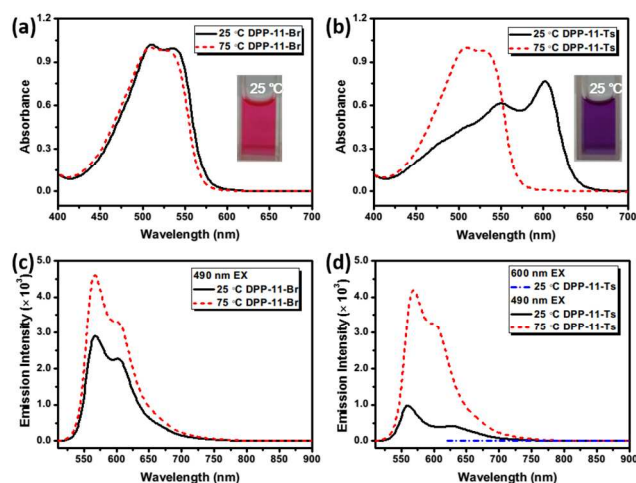
Fig. 3 The absorption of DPP-11-Br (a) and DPP-11-Ts (b) as well as the emission (excited at 490 nm or 600 nm) of DPP-11-Br (c) and DPP-11-Ts (d) at 25 °C and 75 °C. The concentrations of testing aqueous solutions
45 are both 0.1 mM.

The highly ordered molecular arrangement in DPP-11-Ts can be revealed from the temperature-dependent absorption spectra. The absorption band in the range from 400 nm to 700 nm, in Fig 3a-b, is the characteristic absorption of embedded chromophore,
50 DPP. At the temperature of 75 °C, the absorption curves (dash line in Fig3a and 3b) of DPP-11-Br and DPP-11-Ts are exactly the same, corresponding to the color of light pink. As known from DSC in Fig. 2, both DPP-11-Br and DPP-11-Ts are in dissociation state at this temperature, which means this
55 absorption corresponds to the DPP without orientational stacking. At the temperature of 25 °C, both DPP-11-Br and DPP-11-Ts are in aggregated state. The absorption band of DPP-11-Br at low temperature of 25 °C is almost the same as in its dissociation state at high temperature of 75 °C, which suggests that even in the
60 aggregated state of DPP-11-Br, there is no extended orientational stacking between DPP chromophores. However, the absorption spectra of DPP-11-Ts, at the temperature of 25 °C, exhibits significant bathochromic shift corresponding to the blue color of the solution. This striking bathochromic shift suggests that an
65 extended orientational stacking between embedded DPP chromophores is favored by the tosylate ion induced 2D planar structures.

The different extent of orientational stacking between DPP-11-Br and DPP-11-Ts can be clearly indicated from the temperature-
70 dependent emission. The orientational stacking of DPP moieties in the aggregated state of bolaamphiphiles can lead to fluorescence quenching. Larger extent of orientational stacking can result in more significant emission quenching. As shown in Fig. 3c-d, when excited at 490 nm, the emission intensity of
75 aggregated DPP-11-Br at 25 °C is 63% of its intensity in dissociation state at 75 °C; while the emission intensity of aggregated DPP-11-Ts is only 23% of its intensity in the dissociation state. It is noteworthy that the same excited wavelength at 490 nm has been chosen for purpose of parallel
80 comparison. However, as shown in Fig. 3b, rather than the maximum absorption at 490 in dissociation state, the aggregated state of DPP-11-Ts shows maximum absorption at 600 nm. When excited at 600 nm, as shown in Fig. 3d (blue dash), a complete quenching is also observed for aggregated DPP-11-Ts. The much

stronger emission quenching of DPP-11-Ts confirms that the DPP moieties have a larger extent of orientational stacking in the self-assembled 2D planar aggregates.
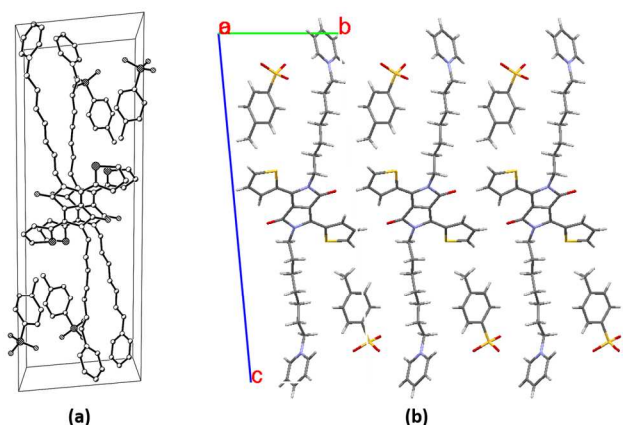
Fig. 4 The crystal structure of DPP-7-Ts, directly crystallized from its concentrated aqueous solution, clearly shows the insertion of tosylate ion at the aggregate-water interface. The hydrophobic segment of this hydrotropic anion prefers to insert into the hydrophobic cavity of aggregates, leaving the polar head towards the water phase.[35]

The crystal structure can also explain the high dissociation temperature and the sharp exothermic peak of DPP-11-Ts solution observed from DSC. However, the single crystal of DPP-11-Ts cannot be prepared due to its long alkyl chains containing eleven carbon atoms. Fortunately, by shortening the chain length to seven carbon atoms, the single crystal of DPP-7-Ts could be obtained.[35] It is noteworthy that this crystal is directly crystallized from its concentrated aqueous solution, and is therefore likely to reflect the molecular arrangement of its aggregates in the solution. As shown in Fig 4, the crystal is made up of numbers of 2D planar monolayers (only one monolayer is shown in Fig. 4b). In each monolayer, the DPPs exhibit an extended orientational stacking along the 2D plane. The crystallized-like arrangement of DPPs should be responsible for the high dissociation temperature. The big exothermic peak in DSC may be ascribed to the breaking up extended stacking between DPPs and the releasing inserted tosylate ions from the aggregate-water interface.

A favorable insertion of hydrotropic anions like tosylate at the aggregate-water interface can be clearly observed from the crystal structure. As shown in Fig 4b, both sides of the 2D planar monolayers are hydrophilic surfaces comprising of cationic pyridinium groups and tosylate ions. Tosylate ion inserts its hydrophobic segment into the hydrophobic cavity of the aggregates, leaving its polar head towards the water phase. This energy favorable orientation makes tosylate prefer to stay at the aggregate-water interface. Comparing with the case of the freely dissolved bromide ion, the inserted tosylate anion can weaken the repulsive force between adjacent cationic head group, favoring an interfaces of low curvature, thus leading to the formation of 2D planar structures.

If the molecular structures of hydrotropic anions don't favor their insertion at the aggregate-water interface, the 2D planar structures as well as the significant bathochromic shift will not be observed. Therefore, we wonder whether we can discover more "effective" hydrotropic anions similar to tosylate ion that can induce the formation of 2D planar structures, just through the

color change of their DPP-11-X solutions. To this end, excess amounts of various salts of hydrotropic anions are added into the solution of DPP-11-Br (1 mM), with a counterion ratio of [X]:[Br] = 2:1. As discussed above, if the solution color remains pink, it suggests no formation of 2D planar structures. If the solution color changes to blue, it suggests that the hydrotropic anion can effectively induce the formation of 2D planar aggregates. In this way, we are able to investigate the relationship between molecular structures of hydrotropic counteranions and their abilities to induce 2D planar structures.
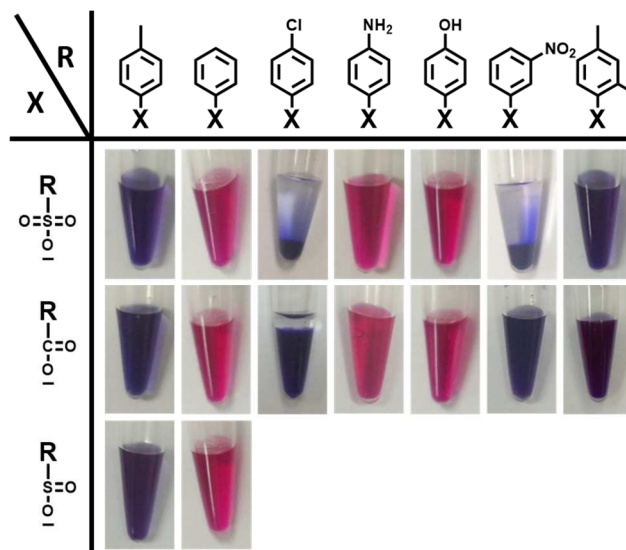
Fig. 5 The organic segment of the hydrotropic anion rather than the polar head determines its ability to induce 2D planar structures. Sodium salts of various hydrotropic anions (X) having the same organic segment, but different polar heads were added into DPP-11-Br aqueous solution (1 mM), with a counterion ratio of [X]: [Br] = 2:1. The color of resulted solutions were recorded here at room temperature.

To understand the effect of polar head of the hydrotropic anions on formation of 2D planar aggregates, we have chosen various hydrotropic anions having the same organic segment, but different polar heads. As shown in Fig. 5, tosylate ion containing a benzyl group and a sulfonate ion can lead to a blue solution. When the polar head is changed to carboxylic ion or sulfinic ion, the resulting color is the same. In another case, using a phenyl group as the organic segment and sulfonate ion as the polar head, the benzenesulfonate ion doesn't cause color change and remains pink, which means that it can't induce the formation of 2D planar structures. Again, when the polar head is changed to carboxylic ion or sulfinic ion, both samples still cannot cause color change, whatever their polar heads are. As shown in Fig. 5, more organic segments like *p*-chlorophenyl, *p*-aminophenyl, *p*-hydroxyphenyl, *m*-nitrophenyl, and 2,4-dimethylphenyl, are tested to support the rule as follows: the ability of a hydrotropic counteranion to induce 2D planar structures is correlated to its organic portion and depends only weakly on its polar head.
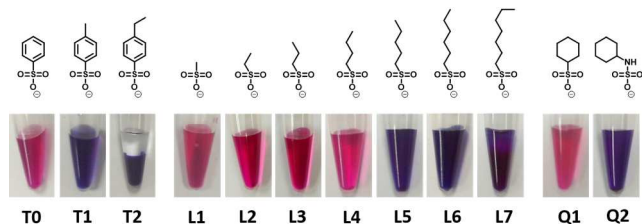
Fig. 6 The size of organic segment of hydrotropic anions should be large enough to induce 2D planar structures. The sodium salts of a series of hydrotropic anions (X), having the same polar segment but different size
5 of organic segments were added into DPP-11-Br aqueous solution (1 mM), with a counterion ratio of [X]: [Br] = 2:1. The color of resulted solutions were recorded here at room temperature.

One may have noted that the difference of only one methyl group between benzenesulfonate and tosylate can lead to totally
10 different aggregation. We wonder if the size of the organic segments plays an important role. To address this point, a series of hydrotropic anions, having the same polar segment but different size of organic segments, are tested by DPP-11-Br. In the first series T0-T2 in Fig. 6, the size of the organic segment is
15 enlarged by gradually increasing the length of alkyl chain

substituted on the phenyl group. T0 cannot lead to color change; while T1, with a little larger size of organic part, does lead to a solution color of blue. Further increasing the size by one methylene, T2 leads to blue as well. It is noteworthy that after
20 addition of T2, phase separation occurs due to the large size of resultant aggregates. Similar phase separation is also observed in Fig. 5. These phenomena suggest that the molecular structures of anions can influence the formation of 2D planar aggregates as well as their growth process.

25 Till now, all the anions we have tested are similar to tosylate ion that contains a rigid aromatic moiety. We wonder whether the aromatic moiety is necessary or not. For this purpose, the hydrotropic anions with only alkyl chain as the organic portion are investigated. As shown in Fig. 6 from L1 to L7, when the
30 carbon number of the alkyl chain is less than five, none of the anions in this series can induce the color change. Only if the carbon number is larger than four, the resultant blue can suggest the formation of 2D planar structures. Therefore, it reveals that the aromatic group is not essential. One more case in series Q1-
35 Q2 further confirms this point. Q1, cyclohexanesulfonic ion, is not able to induce color change; while Q2, cyclamate ion with slightly longer due to the amino group can lead to color change.
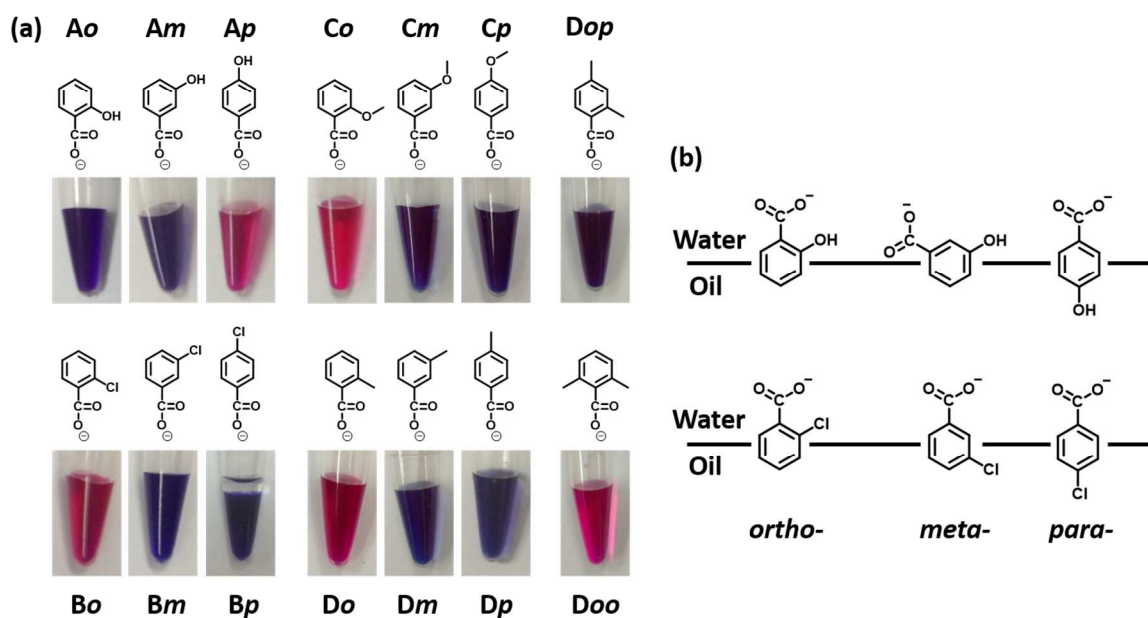
Fig. 7 The hydrophobicity and substituted position of substituents play significant roles in counterion effect. The sodium salts of hydrotropic anions (X),
40 having the same polar segment but different substituted patterns were added into DPP-11-Br aqueous solution (1 mM), with a counterion ratio of [X]: [Br] = 2:1. The color of resulted solutions were recorded here at room temperature. (a). A proposed model to show the microenvironments of inserted anions at the aggregate-water interface (b).

In addition to the size of hydrotropic anions, the substituted pattern including the hydrophobicity of the substituent as well as
45 its substituted position in the aromatic ring can significantly influence the formation of 2D planar aggregates. When the substituent is a hydrophilic one such as hydroxyl group (Ao, Am, Ap in Fig. 7a), the ortho- and meta- substituted anions can induce color change, but the para- substituted one does not work. When
50 the substituent is a hydrophobic one such as chloro group (Bo, Bm, Bp), methoxyl group (Co, Cm, Cp), and methyl group (Do, Dm, Dp), only the ortho- one cannot change the solution color; while the meta- and para- ones can make it. These results suggest

that the microenvironment at the penetration site of counteranion
55 should exert a specific effect. When studying the counterion effect on alkylpyridinium surfactants, Engberts et al.[31] had proposed a model that is helpful for us to interpret this effect as shown in Fig. 7b. In the case of hydrophilic hydroxyl group, the ortho-hydroxyl substituent has the best favorable
60 microenvironment, and the meta- one can rotate itself to achieve a favorable microenvironment, but the para- one can never find a favorable microenvironment when inserted at the aggregate-water interface. That is why only the para-hydroxyl substituent cannot induce formation of 2D planar structures. Similarly, in the case of

hydrophobic substituents, only the ortho- one cannot change the solution color, and the para- one can have the best favorable microenvironment. As a double check, we further test another two samples of Dop and Doo, having one more methyl group at the para- and ortho- position of Do, respectively. Doo bearing two unfavorable ortho- substituents cannot achieve favorable

microenvironment and cannot induce color change as expected. However, Dop, simultaneously having the unfavorable ortho-substituent and the favorable para- substituent, is observed to change the solution color. This suggests that in the case of hydrophobic substituents, the para- substituent may have more power on achieving favorable microenvironment.
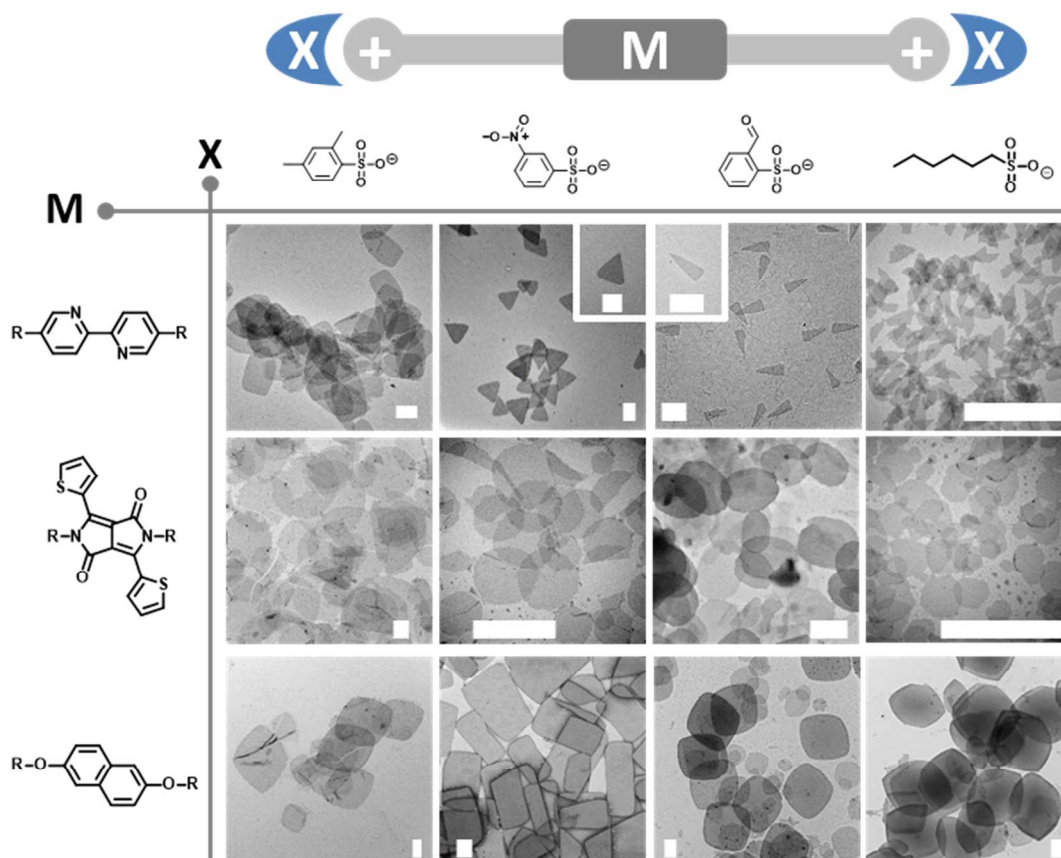
Fig. 8 The molecular structures of the effective counteranion and the embedded conjugated moiety both decide the shape of obtained 2D planar structures. The scale bar is 2 μm.

As more hydrotropic anions have been explored to be able to change the solution color of DPP-11-Br, we wonder whether they can really induce the formation of 2D planar structures. Besides well-studied tosylate ion,[24] the self-assembled structures of another four hydrotropic sulfonic ions with organic segment of 2,4-dimethylphenyl, m-nitrophenyl, o-formylphenyl, and n-hexyl are observed by TEM, as shown in Fig. 8. Firstly, these hydrotropic anions indeed induce the formation of 2D planar structures. Secondly, these anions are not only effective to the bolaamphiphile using DPP as the conjugated core, but also available to other bolaamphiphiles employing other conjugated cores such as dipyridine[27] and naphthalene.[26] Moreover, the size and shape of the obtained 2D planar structures are, amazingly, diverse depending both on the hydrotropic anions and the embedded conjugated cores. For instance, by using dipyridine as the conjugated core, 2,4-dimethylbenzenesulfonic ion leads to a shape of bullet-like; while other ions lead to the shape of triangles. The triangles induced from different ions are also different. For example, the triangle aggregates induced by m-nitrobenzenesulfonic ion is more like an equilateral triangle; while o-formylbenzenesulfonic ion is responsible for the

formation of an isosceles triangle aggregate with an acute vertex angle. If using naphthalene as the conjugated core, m-nitrobenzenesulfonic ion leads to the formation of rectangle aggregates; 2,4-dimethylbenzenesulfonic ion and o-formylbenzenesulfonic ion lead to aggregates with a shape of rhombus or parallelogram; while n-hexanesulfonic ion leads to a shape of hexagon. The diversity of the shape of 2D planar structures may be interpreted from the existence of orientational interactions during the growth of aggregates. In a 2D plane, if the growth rate in each direction is the same or similar, an isotropic shape like circular disk will be formed; if the growth rates are different in different directions due to, for example, orientational stacking of conjugated moieties or orientational dipolar-dipolar interactions of counteranions, an anisotropic shape such as triangle, rectangle, and hexagon can be formed.

Conclusions

In this work, the role of the molecular structures of hydrotropic anions in governing the self-assembled structures of cationic bolaamphiphiles is demonstrated. We reveal that the size and

substituent of the organic segments in hydrotropic anions determine their ability to induce the formation of 2D planar aggregates. Additionally, the shape of 2D planar aggregates is found to be related to the molecular structures of both hydrotropic

5 anions and embedded conjugated moieties, thus resulting in diverse shape of 2D planar structures. With the knowledge of this work, one is able to control the self-assembly of bolaamphiphiles just by easily exchanging counterions, which supplies a simple and feasible way to approach functional supramolecular

10 materials. We have comparatively studied whether the Hofmeister series may play a similar role. However, anions such as SO_4^{2-}, HPO_4^{2-}, COO^-, Cl^-, NO_2^-, CO_3^{2-}, ClO_4^- and OH^- cannot induce the color change as well as the formation of 2D planar aggregates. This confirms our conclusion that the formation of

15 2D planar aggregations indeed relies on the organic segment of hydrotropic anions, on accounts of their ability to penetrate the aggregate-water interface. It should be pointed out that the precise control over the size as well as the size distribution of 2D aggregates still remains a big challenge. It may relates to the

20 dynamic growth of aggregates, influenced by too many factors including the strength of orientational interactions between conjugated group, the dipole of hydrotropic anions, concentration, annealing process, which may eagerly request advances on theory and computation.

25 Experimental Section

General Methods. The thermal data was obtained by the Nano DSC (TA Instruments) differential scanning calorimeter, with a capillary cell volume of 0.3 mL. The heating and cooling scans were performed at a constant scan rate of 1 deg/min. ^{1}H NMR

30 and ^{13}C NMR spectra were recorded on JOEL JNM-ECA300 (300 MHz) apparatuses. ESI-mass spectroscopy measurement was carried out on a PE Sciex API 3000 spectrometer. UV-Vis spectra and Fluorescence spectra were obtained using a Hitachi U-3010 spectrophotometer and Hitachi F-7000

35 spectrofluorometer, respectively, using a cuvette with 1 cm path length, the temperature of which could be controlled by accessional circulating water system. Unless stated, otherwise, 25 °C will be the operating temperature for all experiments.

TEM Measurements and Sample Preparation. TEM was

40 performed on a Hitachi H-7650B operating at an accelerating voltage of 80 kV. 10 μL of the sample solution was applied to a carbon-coated copper grid for 5 min. After removal of excess solution with filter paper, the grid was negatively stained with 10 μL of 1.5% (w/w) uranyl acetate aqueous solution for 1 min. The

45 excess solution was removed by filter paper. The resultant grid was dried in the air for at least one hour.

X-Ray Crystallography. A concentrated solution of DPP-7-Ts with a concentration of 4 mM was heated to 80 °C in water bath. The temperature of water bath was programmed cooled

50 down to 30 °C at a rate of 1 degree per hour. After keeping the solution in water bath for another 12 hours, a needle-like crystal with enough size for X-ray experiment was obtained. The low temperature single-crystal X-ray experiments were performed on a Rigaku Saturn724+ diffractometer with Mo K_α radiation.

55 **Materials and Synthesis.** 1,11-dibromoundecane (96 %), 3,6-di(2-thienyl)-2,5-dihydropyrrolo[3,4-c]pyrrole-1,4-dione (DPP, 95 %) and most of hydrotropic sodium salts were purchased from

TCI; Other hydrotropic sodium salts were purchased from J&K. All of compounds were used as received. The deionized water

60 was obtained from Milli-Q Advantage A10. The synthesis of DPP-7-Ts, DPP-11-Ts, and bolaamphiphiles containing dipyridine and naphthalene can be referred to our previous work.[23,26,27] The synthesis of DPP-11-Br is described in Scheme 1 as follows:

65
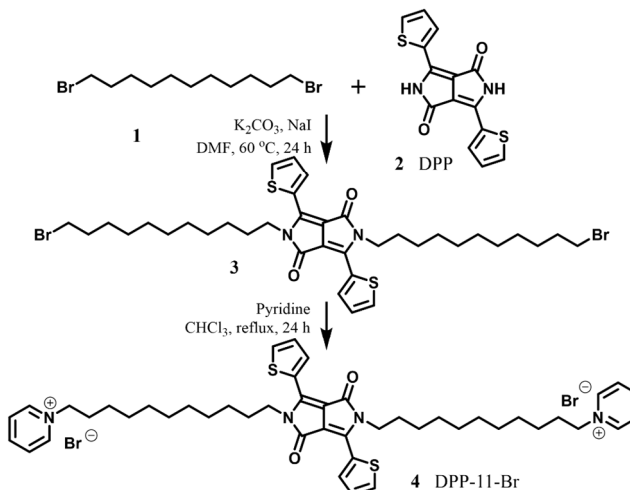
Scheme 1 Synthesis of DPP-11-Br.

Synthesis of DPP derivative 3: 1,11-dibromoundecane **1** (1.82 g, 5.79 mmol), K_2CO_3 (0.435 g, 3.15 mmol), and NaI (0.47 g, 3.15 mmol) were added to a solution of DPP **2** (0.435 g, 1.45

70 mmol) in dry DMF (14 mL). The mixture was stirred at 60 °C for 24 h. After cooling to room temperature, the mixture was poured into water and extracted with ethyl acetate. The organic phase was dried over $MgSO_4$, and the solvent was evaporated in vacuum. The product **3** (0.22 g, 20 %) was obtained by column

75 chromatography (silica, eluent CH_2Cl_2–heptane 70–30). ^{1}H NMR (300 MHz, $CDCl_3$, 28 °C, tetramethylsilane (TMS), ppm): δ 8.93 (d, ^3J(H,H) = 4.8 Hz, 2H), 7.64 (d, ^3J(H,H) = 3.9 Hz, 2H), 7.29 (t, ^3J(H,H) = 4.8 Hz, 2H), 4.07 (t, ^3J(H,H) = 7.8 Hz, 4H), 3.4 (t, ^3J(H,H) = 6.8 Hz, 4H), 1.84 (m, 4H; CH_2CH_2Br), 1.74 (m, 4H;

80 CH_2CH_2DPP), 1.27 (m, 28H); ^{13}C NMR (75 MHz, $CDCl_3$, ppm) δ 161.5, 140.2, 135.4, 130.8, 130.0, 128.8, 107.8, 42.4, 34.2, 33.0, 30.1, 29.6, 29.6, 29.5, 29.4, 28.9, 28.3, 27.0; MS (ESI[+]) calcd: 766; found: *m/z* 767 [MH][+].

Synthesis of DPP-11-Br 4: Dry pyridine (5 mL) was added to a

85 solution of **3** (0.12 g, 0.16 mmol) in dry chloroform (10 mL). The solution was refluxed under nitrogen for 24 h. After cooling the mixture to room temperature, it was added dropwise to toluene (100 mL). The resulting red precipitate was dissolved in methanol and further purified by precipitating in diethyl ether affording **4**

90 with high purity (0.122 g, 87 %). ^{1}H NMR (300 MHz, CD_3OD, 28 °C, TMS, ppm): δ 9.11 (d, ^3J(H,H) = 5.6 Hz, 4H; 2-H, 6-H Py), 8.80 (d, ^3J(H,H) = 4.3 Hz, 2H; 3-H Th), 8.65 (t, ^3J(H,H) = 7.6Hz, 2H; 4-H Py), 8.17 (t, ^3J(H,H) = 7.0 Hz, 4H; 3-H 5-H Py), 7.85 (d, ^3J(H,H) = 4.8 Hz, 2H; 5-H Th), 7.24 (t, ^3J(H,H) = 4.32

95 Hz, 2H; 4-H Th), 4.7 (t, ^3J(H,H) = 7.4 Hz, 4H; CH_2Py), 3.93 (t, ^3J(H,H) = 7.3 Hz, 4H; CH_2DPP), 2.03 (m, 4H; CH_2CH_2Py), 1.62 (m, 4H; CH_2CH_2DPP), 1.26 (m, 28H; $CH_2CH_2(CH_2)_7CH_2CH_2$); ^{13}C NMR (75 MHz, CD_3OD, ppm) δ 162.3, 146.8, 145.9, 141.2, 136.5, 133.1, 130.6, 129.5, 108.4, 63.1, 43.1, 32.5, 30.8, 30.5,

30.5, 30.2, 30.1, 29.9, 27.8, 27.2; MS (ESI$^+$) calcd: 924; found: m/z 845 [M- Br]$^+$.

Acknowledgements

Notes and references

^{a} MOE Key Lab of Organic Optoelectronics & Molecular Engineering Department of Chemistry, Tsinghua University Beijing 100084 (China). Fax: (+86) 10-6277-1149; Tel: (+86) 10-6279-6283; E-mail: xi@mail.tsinghua.edu.cn

^{b} Department of Chemistry Katholieke Universiteit Leuven Celestijnenlaan 200F, B-3001 Leuven (Belgium).

† Electronic Supplementary Information (ESI) available: NMR and Mass for DPP-11-Br. For crystallographic data in CIF or other electronic format See DOI: 10.1039/b000000x/

1. J.-H. Fuhrhop and T. Wang, *Chem. Rev.*, 2004, **104**, 2901–2938.
2. A. Meister and A. Blume, *Curr. Opin. Colloid Interface Sci.*, 2007, **12**, 138–147.
3. T. Benvegnu, M. Brard, and D. Plusquellec, *Curr. Opin. Colloid Interface Sci.*, 2004, **8**, 469–479.
4. R. Nagarajan, *Chem. Eng. Commun.*, 1987, **55**, 251–273.
5. E. L. Chang, *Biochem. Biophys. Res. Commun.*, 1994, **202**, 673–679.
6. M. De Rosa, E. Esposito, A. Gambacorta, B. Nicolaus, and J. D. Bu'Lock, *Phytochemistry*, 1980, **19**, 827–831.
7. M. De Rosa, A. Gambacorta, and A. Gliozzi, *Microbiol. Rev.*, 1986, **50**, 70–80.
8. Y. Okahata and T. Kunitake, *J. Am. Chem. Soc.*, 1979, **101**, 5231–5234.
9. K. Köhler, G. Förster, A. Hauser, B. Dobner, U. F. Heiser, F. Ziethe, W. Richter, F. Steiniger, M. Drechsler, H. Stettin, and A. Blume, *Angew. Chem. Int. Ed.*, 2004, **43**, 245–247.
10. B. Song, Z. Wang, and X. Zhang, *Pure Appl. Chem.*, 2006, **78**, 1015–1023.
11. B. Song, G. Q. Liu, R. Xu, S. C. Yin, Z. Q. Wang, and X. Zhang, *Langmuir*, 2008, **24**, 3734–3739.
12. T. Y. Wang, J. Jiang, Y. Liu, Z. B. Li, and M. H. Liu, *Langmuir*, 2010, **26**, 18694–18700.
13. G. Yu, C. Han, Z. Zhang, J. Chen, X. Yan, B. Zheng, S. Liu, and F. Huang, *J. Am. Chem. Soc.*, 2012, **134**, 8711–8717.
14. X. Yan, S. Li, T. R. Cook, X. Ji, Y. Yao, J. B. Pollock, Y. Shi, G. Yu, J. Li, F. Huang, and P. J. Stang, *J. Am. Chem. Soc.*, 2013, **135**, 14036–14039.
15. F. Li, Q. Song, L. Yang, G. Wu, and X. Zhang, *Chem. Commun.*, 2013, **49**, 1808–1810.
16. T. Shimizu, M. Kogiso, and M. Masuda, *Nature*, 1996, **383**, 487–488.
17. H. Shao, J. Seifert, N. C. Romano, M. Gao, J. J. Helmus, C. P. Jaroniec, D. A. Modarelli, and J. R. Parquette, *Angew. Chem. Int. Ed.*, 2010, **49**, 7688–7691.
18. K. Köhler, G. Förster, A. Hauser, B. Dobner, U. F. Heiser, F. Ziethe, W. Richter, F. Steiniger, M. Drechsler, H. Stettin, and A. Blume, *J. Am. Chem. Soc.*, 2004, **126**, 16804–16813.
19. Y. Yan, T. Lu, and J. Huang, *J. Colloid Interface Sci.*, 2009, **337**, 1–10.
20. Y. Yao, M. Xue, J. Chen, M. Zhang, and F. Huang, *J. Am. Chem. Soc.*, 2012, **134**, 15712–15715.
21. L. Gao, B. Zheng, Y. Yao, and F. Huang, *Soft Matter*, 2013, **9**, 7314–7319.
22. Y. Yao, X. Chi, Y. Zhou, and F. Huang, *Chem. Sci.*, 2014, DOI: 10.1039/c4sc00585f.
23. B. Song, Z. Wang, S. Chen, X. Zhang, Y. Fu, M. Smet, and W. Dehaen, *Angew. Chem. Int. Ed.*, 2005, **44**, 4731–4735.
24. G. Wu, P. Verwilst, K. Liu, M. Smet, C. F. J. Faul, and X. Zhang, *Chem. Sci.*, 2013, **4**, 4486–4493.
25. J. Huang, S. Wang, G. Wu, L. Yan, L. Dong, X. Lai, S. Yin, and B. Song, *Soft Matter*, 2014, **10**, 1018–1023.
26. K. Liu, C. Wang, Z. Li, and X. Zhang, *Angew. Chem. Int. Ed.*, 2011, **50**, 4952–4956.
27. G. Wu, P. Verwilst, J. Xu, H. Xu, R. Wang, M. Smet, W. Dehaen, C. F. J. Faul, Z. Wang, and X. Zhang, *Langmuir*, 2012, **28**, 5023–5030.
28. T. K. Hodgdon and E. W. Kaler, *Curr. Opin. Colloid Interface Sci.*, 2007, **12**, 121–128.
29. J. Eastoe, M. H. Hatzopoulos, and P. J. Dowding, *Soft Matter*, 2011, **7**, 5917–5925.
30. R. Abdel-Rahem, *Adv. Colloid Interface Sci.*, 2008, **141**, 24–36.
31. K. Bijma and J. B. F. . Engberts, *Langmuir*, 1997, **13**, 4843–4849.
32. K. Bijma, M. J. Blandamer, and J. B. F. N. Engberts, *Langmuir*, 1998, **14**, 79–83.
33. K. Bijma, E. Rank, and J. B. F. N. Engberts, *J. Colloid Interface Sci.*, 1998, **205**, 245–256.
34. Y. Lin, Y. Qiao, X. Cheng, Y. Yan, Z. Li, and J. Huang, *J. Colloid Interface Sci.*, 2012, **369**, 238–244.
35. Crystal data for DPP-7-Ts: C$_{38}$H$_{44}$N$_4$O$_2$S$_2$-2(CH$_3$C$_6$H$_4$SO$_3$), M = 995.26, triclinic, a = 9.371(2) Å, b = 9.447(2) Å, c = 27.755 (7) Å, α = 84.533(6)°, β = 83.630(7)°, γ = 88.365(9)°, V = 2430.4(10) Å^3, T = 153(2) K, space group P$\bar{1}$, Z = 2, μ(MoKα) = 0.519 mm^{-1}, 24761 reflections measured, 8586 independent reflections (R_{int} = 0.1268). The final R_1 values were 0.0952 ($I > 2\sigma(I)$), The final $wR(F^2)$ values were 0.1939 ($I > 2\sigma(I)$). The final R_1 values were 0.1244 (all data), The final $wR(F^2)$ values were 0.2138 (all data). The goodness of fit on F^2 was 1.152. CCDC number: CCDC 992925.